CMLS, Cell. Mol. Life Sci. 61 (2004) 1532–1542
1420-682X/04/121532-11
DOI 10.1007/s00018-004-4082-3


CMLS Cellular and Molecular Life Sciences

# Research Article

# Differential distribution of TASK-1, TASK-2 and TASK-3 immunoreactivities in the rat and human cerebellum

**Z. Rusznák[a,*], K. Pocsai[a], I. Kovács[b], Á. Pór[a], B. Pál[a], T. Bíró[a] and G. Szücs[a]**

[a] Department of Physiology, Medical and Health Science Centre, University of Debrecen, P.O. Box 22, 4012 Debrecen, (Hungary), Fax: + 36 52 432 289, e-mail: rz@phys.dote.hu
[b] Department of Pathology, HBM Kenézy Gyula County Infirmary, Bartók Béla u. 2-26., 4043 (Hungary)

Received 25 February 2004; received after revision 19 April 2004; accepted 28 April 2004

**Abstract.** In this work, the distributions of some acid-sensitive two-pore-domain $K^+$ channels (TASK-1, TASK-2 and TASK-3) were investigated in the rat and human cerebellum. Astrocytes situated in rat cerebellar tissue sections were positive for TASK-2 channels. Purkinje cells were strongly stained and granule cells and astrocytes were moderately positive for TASK-3. Astrocytes isolated from the hippocampus, cerebellum and cochlear nucleus expressed TASK channels in a primary tissue culture. Our results suggest that TASK channel expression may be significant in the endoplasmic reticulum of the astrocytes. The human cerebellum showed weak TASK-2 immunolabelling. The pia mater, astrocytes, Purkinje and granule cells demonstrated strong TASK-1 and TASK-3 positivities. The TASK-3 labelling was stronger in general, but it was particularly intense in the Purkinje cells and pia mater.

**Key words.** TASK immunopositivity; astrocyte culture; cerebellum; endoplasmic reticulum; human brain.

## Introduction

Based upon sequence similarities between the pore-forming (or $\alpha$) subunits of the $K^+$ channels, three major classes (known as superfamilies) are distinguished. Besides the voltage-gated and inward rectifier $K^+$ channels [for reviews see 1, 2], a new superfamily with four transmembrane domains has been described more recently [3]. In these channels, the functional channel is a dimer [4], where the subunits consist of a tandem of pore-forming domains; hence these channels are often referred to as tandem-pore-domain (TPD), two-P or PP domain channels. Several classes of the TPD channels have been described in the past few years and more recently (TWIK [4–6], TREK [7–10], TRAAK [11], TASK [12–19], TALK [20, 21], THIK [22] and TRESK [23]) and the number is continuously growing. Regulation of these channels seems to be extraordinarily complex, as they may be gated by mechanical stretch of the membrane, heat, free fatty acids, volatile anaesthetics, protein kinases and various other chemical stimuli, including the alteration of the intra- or extracellular pH.

TASK (or TWIK-related acid sensitive $K^+$) channels are particularly sensitive to changes in the extracellular pH [12, 13, 15, 19]. Certain members of the TASK family (TASK-1, TASK-3 and TASK-5) are more closely related to each other than to TASK-2 and TASK-4. In fact, the latter two channels are now classified as members of the TALK (TWIK-related alkaline-pH-activated $K^+$ channel) group, and TASK-4 is often referred to as TALK-2 [20, 21].

TASK (and in particular TASK-1) channels are generally accepted to function as 'background' $K^+$ channels [12], being responsible for the high $K^+$ conductance of the various cells at rest, crucially determining, therefore, their resting membrane potential. The standing outward $K^+$ current of

* Corresponding author.

cerebellar granule cells ($I_{Kso}$; [24]) is also generated by the activity of TASK-1 channels [25]. Moreover, a recent study has demonstrated that TASK-3 channels play crucial roles in the $K^+$-dependent apoptosis of cerebellar granule neurones in culture [26]. Considering the broad physiological functions of the TASK channels, it is not surprising that the presence of TASK-specific nucleic acid sequences has been reported in several different tissues, such as brain, lung, testis, pancreas and kidney [19, 27]. Besides physiological functions, TASK-3 channels may have oncogenic potential [28] and increased expression of the TASK-3 encoding KCNK9 gene has been reported in a significant portion of breast cancers [29].

When the distribution of TASK channels in the central nervous system was investigated, some rather interesting experimental results were obtained. In human brain, both TASK-1- and TASK-3-specific mRNA was noticed in a crude extract, in contrast to the almost complete lack of TASK-2 mRNA [27]. On the other hand, using immunohistochemical methods, both TASK-1 [30] and TASK-2 immunopositivities [31] were observed in the central nervous system of the rat. Particularly noteworthy is that while neurones, glial cells and ependymal cells all expressed TASK-1 channels, TASK-2 positivity was reported on neurones only and neither glial nor ependymal cells showed noticeable TASK-2 immunopositivity. These data suggested that there might be significant differences in the tissue distribution of the various TASK channels even within the same species. As for the human brain, the data available concern the presence (or absence) of TASK-specific mRNA, and this cannot provide information about the localisation of TASK channels at the cellular level, hence a more detailed investigation of the distribution of TASK-specific immunreactivity seems to be important in the human central nervous system.

In the present study, we demonstrate the immunohistochemical distribution of TASK-1, TASK-2 and TASK-3 in the human cerebellum, and an interspecies comparison is performed between human and rat. Moreover, using rat astrocytes maintained in tissue culture, we provide evidence that both GluR- and GluT-type astrocytes express strong TASK-1 immunoreactivity. Somewhat weaker but nevertheless present TASK-2 and TASK-3 immunoreactions were also found in both types of astrocyte. The results obtained in astrocyte tissue culture were confirmed by Western blotting and RT-PCR methods.

## Materials and methods

### Enzymatic isolation and tissue culture of astrocytes

The enzymatic dissociation of the hippocampus, cerebellum and cochlear nucleus was performed using a technique similar to that described earlier [32] (the procedure was authorised by the Ethical Committee of the University of Debrecen). In short, 3- to 8-day-old Wistar rats were decapitated, their brain removed in ice-cold dissecting medium (D1; in mM: NaCl, 136; KCl, 5.2; $Na_2HPO_4 \cdot H_2O$, 0.64; $KH_2PO_4$, 0.22; glucose, 16.6; sucrose, 22; HEPES, 10; plus 0.06 U/ml penicillin and 0.06 µg/ml streptomycin). All chemicals were purchased from Sigma (St. Louis, Mo.), unless stated otherwise. Enzymatic dissociation of brain tissue was achieved by employing D1 solution containing trypsin (0.025 g/ml; 30 min, 37 °C). At the end of the incubation period, the now gelatinous tissue pieces were transferred to minimum essential medium (MEM) supplemented with 10% fetal calf serum (FCS) for 5 min (room temperature). Individual cells were obtained by applying very gentle agitation with fire-polished Pasteur pipettes. The cell suspension was diluted for a density of 100,000 cells/ml, and 0.5 ml of this suspension was transferred onto cover-slips situated in 12 wells of a 24-well tray (the marginal wells were not used in order to reduce the risk of infection). The cells were allowed to grow at 37 °C in a 5% $CO_2$ atmosphere. The feeding medium (MEM supplemented with 10% FCS) was changed on the following day and every other day thereafter. Under these conditions most of the neurones died, while the astrocytes kept on dividing and growing. Immunocytochemistry was usually conducted on 4- to 5-day-old cultures by which time 70–80% confluence was reached.

### Fluorescent immunochemistry

Fluorescent immunochemistry was employed on astrocyte cultures. Prior to the immunochemistry, the cells were fixed with 4% paraformaldehyde (15 min, room temperature), then washed with phosphate-buffered saline (PBS) containing 100 mM glycine. Permeabilisation was carried out by bathing the cells in PBS containing Triton X-100 (0.1%) for 10 min followed by washing with PBS. Aspecific binding was prevented by incubating the cells in PBS containing bovine serum albumin (BSA, 1%) for 30 min. The cells were then incubated with the primary antibodies (table 1) for 60 min at room temperature or overnight at 4 ºC. The cells were rinsed in PBS (3 × 5 min), incubated with the appropriate secondary antibody (table 2) for 60 min at room temperature, followed by rinsing in PBS again (3 × 5 min). At the end of the procedure, the nuclei were stained with DAPI followed by cover-slip mounting.

### Non-fluorescent immunostaining

When tissue samples from rat or human cerebellum were investigated, non-fluorescent immunohistochemistry was used. Formaldehyde-fixed, paraffin-embedded sections were prepared from the human tissue, while both formaldehyde-fixed (24 h) and frozen (in liquid nitrogen) sections were employed for rat cerebellum. The human cerebellar tissue blocks were obtained from the histo-

Table 1. List of the primary antibodies employed.

| Antibody | Specificity | Dilution | Raised in | Obtained from |
|---|---|---|---|---|
| Anti-TASK-1 | rat | 1:50; 1:500; 1:1000 | rabbit | Alomone, Jerusalem, Israel |
| Anti-TASK-2 | rat | 1:50 | rabbit | Alomone |
| Anti-TASK-1 | human | 1:10 | goat | Santa Cruz, Calif. |
| Anti-TASK-2 | rat, human | 1:10 | goat | Santa Cruz |
| Anti-TASK-3 | rat, human | 1:10 | goat | Santa Cruz |
| Anti-GFAP | human | 1:400 | rabbit | DAKO, Glostrup, Denmark |
| Anti-GFAP | rat, human | 1:100 | goat | Santa Cruz |
| Anti-NFP | human | 1:50 | mouse | DAKO |

GFAP, glial fibrillary acidic protein; NFP, neurofilament protein.

pathology specimen of a 78-year-old female patient dying as a consequence of acute cardiac failure (the tissue sample was obtained with the written approval of the patient's husband and daughter, the procedure was also authorised by the Ethical Committee of the University of Debrecen). The basic steps of the immunostaining were the same for both the frozen sections and formaldehyde-fixed, paraffin-embedded slices. In the cases of formaldehyde-fixed sections, antigen retrieval (AR) was achieved using either pronase treatment (0.1%, 3 min) or by incubating the tissue specimen in 0.01 M Tris buffer (pH 8.8) in a microwave oven (3 × 5 min).

Following AR, the endogenous peroxidase activity was blocked by 3% $H_2O_2$ solution (10 min, room temperature). Aspecific binding was prevented by incubating the cells with Protein Block Serum Free Reagent (DAKO, 10 min, room temperature) followed by washing with PBS. The tissue sections were then exposed to the appropriate primary antibody (60 min; table 1) followed by rinsing with PBS (3 × 5 min), the application of the biotin-labelled secondary antibody (30 min; table 2) and rinsing with PBS again at room temperature. The tissue samples were then exposed to horseradish peroxidase-conjugated streptavidin (streptavidin/HRP; 1:500; room temperature) for 30 min, rinsed with PBS, then incubated with alkaline phosphatase-conjugated streptavidin (1:50; 30 min). The immunoreaction was visualised using either VIP (SK4600; Vector) or a diamino-benzidine kit (DAB; Vector). At this point, the procedure was either terminated with the application of a slight counterstaining (haematoxylin) or the slices were subjected to another, glia- or neurone-specific immunoreaction. In these cases, the blocking solution was employed again for 10 min, followed by the application of the second primary antibody (30 min). The sections were rinsed in Tris-buffered saline (TBS) both prior to and after the application of the secondary antibodies (30 min, room temperature). The samples were then incubated in alkaline phosphatase-conjugated streptavidin (1:50; 30 min), and the immunoreaction was visualised using New Fuchsin.

In cases where primary antibodies raised in rabbit were used in the cerebellar sections, the EnVision visualisation method (DAKO) was also used. The immunoreactions were investigated employing a Nikon Eclipse 600W microscope (Nikon, Tokyo, Japan), equipped with an RT Color CCD camera. The images were acquired and processed using the Spot RT v3.5 software. Pixel analysis was performed using the Image-Pro Plus software. Confocal microscopy images were acquired using a Zeiss LSM 510 microscope (Oberkochen, Germany).

Table 2. List of the secondary antibodies employed.

| Antibody | Dilution | Obtained from |
|---|---|---|
| Anti-rabbit FITC | 1:200 | Vector, Burlingame, Calif. |
| Anti-goat FITC | 1:200 | Vector |
| Anti-goat Texas Red | 1:200 | Vector |
| Anti-goat biotin | 1:500 | DAKO |
| Anti-rabbit biotin | 1:300 | DAKO |
| Anti-mouse biotin | 1:300 | DAKO |

**Transfection of the cultured astrocytes**

In some cases, the astrocytes maintained in tissue culture were transfected with the pDsRed2-ER vector (BD Biosciences, Palo Alto, Calif.) when the culture was 50% confluent. This vector (size: 4.7 kb) was designed for fluorescent labelling of the endoplasmic reticulum (ER) in living cells [33, 34]. The DNA sequence encodes a red fluorescent protein, an ER-targeting sequence and an ER retention sequence. The astrocyte culture was fixed in formaldehyde 24 h after the transfection, and the immunolabelling of the TASK channels was performed as described before. The red fluorescence clearly indicated the ER in those cells where the transfection was successful.

**Reverse transcription PCR**

The expression of mRNA for TASK-1, -2 and -3 in cultured rat astrocytes was determined by RT-PCR. Total RNA was extracted from the cultured astrocytes using TRIzol (Invitrogen, Paisley, UK) following the manufacturer's procedure. Usually, 3 µg RNA was reverse transcribed with 5 mM $MgCl_2$, 1× reverse transcription buffer (10 mM Tris-HCl, 50 mM KCl, 0.1% Triton X-100, pH 9 at 25 °C),

1 mM dNTP mix, 1 U/µl recombinant RNasin RNAse inhibitor, 15 U/µl AMV reverse transcriptase and 0.5 µg oligo(dT)$_{15}$ primers (all from Promega, Mannheim, Germany). Subsequent PCR amplification (95 °C for 5 min; 35 cycles of 95 °C for 1 min, 58 °C for TASK-1 or 65 °C for TASK-2 and TASK-3 for 1 min, 72 °C for 1 min; 4 °C for 5 min) was performed on the GeneAmp PCR System 2400 (Perkin Elmer Wellesley, Mass.) with the following primers (all from Invitrogen): TASK-1, 5′-CAC CGT CAT CAC CAC AAT CG-3′ and 5′-TGC TCT GCA TCA CGC TTC TC-3′ (predicted size, 515 bp); TASK-2, 5′-TGG GCG CCT CTT CTG TGT CTT CTA-3′ and 5′-TCC CCT CCC CCA CTT GTT TTC ATT-3′ (predicted size, 629 bp); TASK-3, 5′-ATG AGA TGC GCG AGG AGG AGA AAC-3′ and 5′-ACG AGG CCC ATG CAA GAA AAG AAG-3′ (predicted size, 414 bp) [35]. The PCR products were visualized on a 2% agarose gel with ethidium bromide and visualized by Image-Pro Plus software (Media Cybernetics, Silver Spring, Md.).

### Western blotting

Cultured astrocytes were washed with ice-cold PBS, harvested in homogenization buffer [20 mM TRIS-HCl, 5 mM EGTA, 1 mM 4-(2-aminoethyl)benzenesulfonyl fluoride, 20 µM leupeptin, pH 7.4; all from Sigma] and disrupted by sonication on ice [36]. The protein content of samples was measured by a modified BCA protein assay (Pierce, Rockford, Ill.). Total cell lysates were mixed with SDS-PAGE sample buffer and boiled for 10 min at 100 °C. The samples were subjected to SDS-PAGE according to Leammli [37] (8% gels were loaded with 20–30 µg protein per lane) and transferred to nitrocellulose membranes (BioRad, Vienna, Austria). Membranes were then blocked with 5% dry milk in PBS and probed with goat polyclonal primary antibodies against TASK-1, -2, or -3 (all from Santa Cruz). A peroxidase-conjugated rabbit anti-goat IgG antibody (BioRad) was used as a secondary antibody and signals were then amplified using an anti-rabbit Vectastain ABC kit (Vector). In control experiments, specificity of staining was assessed by incubating the membrane with antibodies pre-absorbed with the corresponding synthetic blocking peptides (Santa Cruz), a procedure which completely prevented the immunosignal in all cases (data not shown). The immunoreactive bands were visualised by an ECL Western blotting detection kit (Amersham, Little Chalfont, UK) on light-sensitive films (AGFA, Brussels, Belgium).

## Results

### TASK-channel-specific immunoreactions in the rat cerebellum

Figure 1 demonstrates the TASK immunopositivity pattern observed in the cerebellum of the rat. Figure $A_1$, $B_1$ and $C_1$ show the results of TASK-1, TASK-2 and TASK-3 immunopositivities, respectively, in paraffin-embedded sections. The Purkinje cells and the pia mater showed particularly strong TASK-1 positivity (fig. $1A_1$), although the molecular and granule cell layers were also clearly positive. (Note that the distribution of TASK-1 immunoreaction has already been reported by Kindler et al. [30] and is presented here for direct comparison of the immunopositivity pattern of the TASK-1, -2 and -3 channels in the rat cerebellum and between the rat and human cerebellum.) TASK-2 immunoreactivity (which was previously studied by Gabriel et al. [31]) was somewhat weaker (fig. $1B_1$), especially in the cases of the pia mater Purkinje cells and granule layer. TASK-3 immunopositivity could also be detected in the rat cerebellum (fig. $1C_1$). Similar to the TASK-1 and TASK-2 immunoreactions, Purkinje cells showed distinct positivity for TASK-3, which was also found in the molecular and granule cell layers, while the pia mater did not seem to express TASK-3 channels at all. Strong TASK-3 positivity could be detected in the white matter of the rat cerebellum. Interestingly, a small portion of the Purkinje cells showed only weak or no immunopositivity for TASK-1 and TASK-2. Although uneven distribution of the TASK-specific antibodies cannot be ruled out completely as the reason for this finding, the markedly positive immunoreaction of the neighbouring Purkinje cells makes this possibility very unlikely. In fact, this finding might suggest that the Purkinje cells are not uniform in terms of TASK channel expression.

As figure $1A_2$, $1B_2$ and $1C_2$ demonstrate, TASK channel expression of the cerebellar astrocytes was also investigated. In these experiments 4-µm-thick frozen sections were prepared and glial fibrillary acidic protein (GFAP) TASK double staining was performed, because the application of the GFAP-specific antibody allowed the identification of the astrocytes in the tissue sections. In these images, some spider-like, GFAP-positive (purple) cells were clearly seen showing simultaneous TASK-1, -2 or -3 positivity (brown). Figure $1A_3$, $1B_3$ and $1C_3$ illustrate some astrocytes shown in the previous column of images at higher magnification.

Generally, the validity of the positive immunoreactions was confirmed in two ways. In some experiments, the primary antibodies were omitted from the solution to check for the presence of non-specific binding of the secondary antibody. Moreover, in a different set of experiments, the primary antibodies were pre-incubated with their blocking peptides. Neither the former, nor the latter procedure resulted in appreciable immunopositivity (see below).

### TASK-channel-specific immunoreactions on cultured astrocytes

The TASK- and GFAP-specific immunoreactions indicated that the astrocytes of the rat cerebellum express all

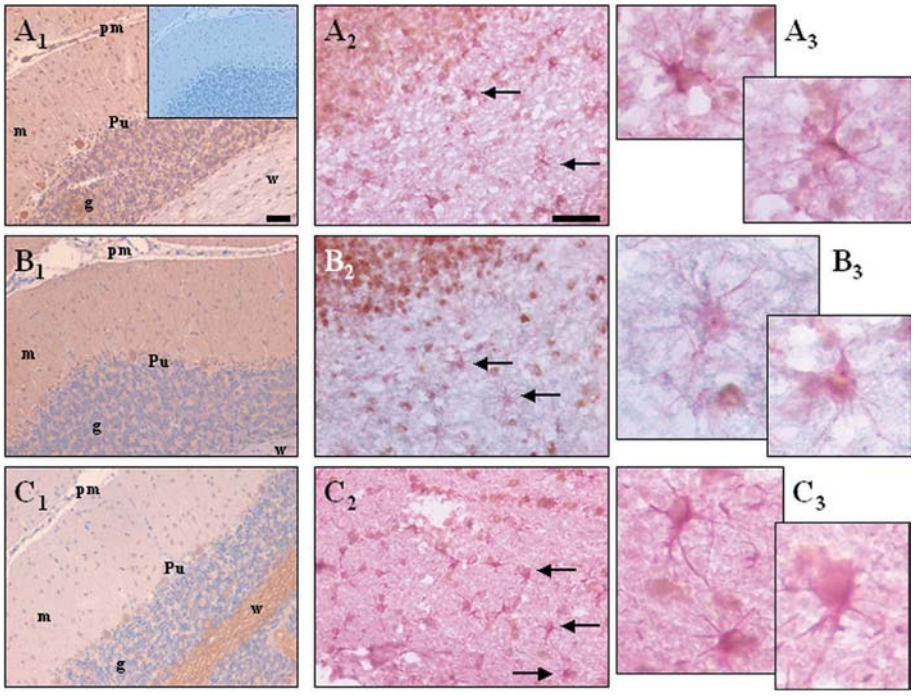


Figure 1. TASK immunoreactivity in the cerebellum of the rat. ($A_1$) Formalin-fixed, paraffin-embedded histological section demonstrating TASK-1 immunoreactivity (brown). The specimen was counterstained with haematoxylin. The molecular layer, granule layer and Purkinje cells are clearly positive. ($A_2$) Frozen section, demonstrating TASK-1 (brown) and GFAP (purple) positivity. No counterstaining was performed. Arrows indicate some astrocytes showing both GFAP and TASK positivities. ($A_3$) The same cells at higher magnification. The structure of panels *B* and *C* are the same but show TASK-2 and TASK-3 immunoreactivities, respectively. Scale bars; 40 µm. pm, pia mater; g, granule layer; m, molecular layer; w, white matter; Pu, Purkinje layer. The inset in $A_1$ shows the result of the procedure in the absence of the primary antibody.

three types of TASK channel. In the next step, astrocytes were maintained in a primary tissue culture, and the expression of the TASK channels was investigated under these conditions as well. As figure 2D demonstrates, the cells could be identified as astrocytes on the basis of their GFAP positivity. Note that in the absence of the primary antibody, only the nuclei of the cells could be identified, and no FITC positivity could be observed (insets). When anti-TASK-1, -TASK-2 and -TASK-3 antibodies were tried in these astrocyte cultures, positive immunoreaction could be observed in all three cases (fig. 2A–C), similar to our findings in cerebellar tissue sections. The intensity of the TASK-1 immunoreaction was the strongest, while TASK-2 and TASK-3 gave less powerful immunolabelling [although they were much more intense than the immunoreaction observed in the presence of the blocking peptide (see insets) or in the absence of the primary antibody (not shown)]. Note that the image seen in figure 2B was taken with a longer exposure time than those demonstrated in figure 2A, C.

In the cell cultures, two types of astrocyte could be clearly distinguished (figs. 2, 3). One type possessed numerous thin processes and a relatively small cell body, which gave the cell a rather characteristic, star-like appearance. These cells showed strong GFAP positivity, and they were

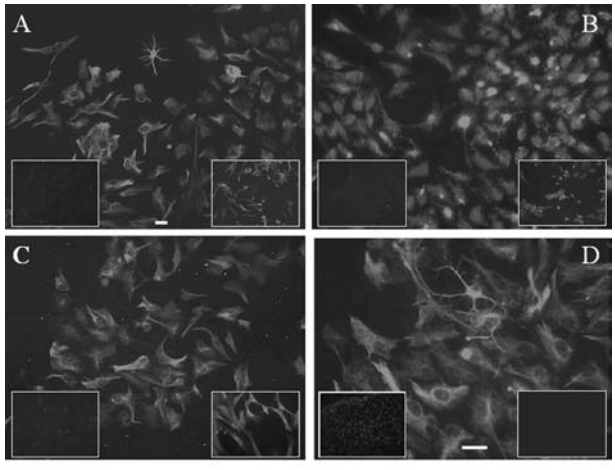


Figure 2. TASK immunoreactivity of rat cerebellar astrocytes maintained in tissue culture. TASK-1 (*A*), TASK-2 (*B*) and TASK-3 (*C*) immunolabelling, all at the same magnification. The insets of each panel show the result of an immunising peptide block (left; blocking peptide concentration 7 µg/ml for TASK-1 and TASK-2, 20 µg/ml for TASK-3) and the specific reactions in astrocyte cultures obtained from the cochlear nucleus (right). (*D*) Result of the glia-specific (anti-GFAP) immunoreaction. The insets show the DAPI labelling of the nuclei (on the left) as well as the experimental result when no primary antibody was employed (on the right; both insets show the same field of view). Scale bars, 20 µm.

identified as GluT cells [38]. The other cell type gave a somewhat weaker GFAP immunoreaction, possessed many fewer and shorter processes, and had a characteristic brick-like shape. On the basis of the morphological features of the latter cell type and the less intense GFAP positivity, these cells corresponded to GluR astrocytes [38]. Regardless of the origin of the cell cultures, GluT cells showed more intense TASK-1 positivity than the GluR astrocytes (see fig. 2A). No such difference could be observed in the cases of the TASK-2 and TASK-3 immunoreactions, but this may be explained by the generally weaker immunopositivities for these antibodies.

Astrocyte cultures were also prepared using cells isolated from the cochlear nuclei and the hippocampus of the rats, and these cultures behaved in the same way as cerebellar astrocytes, suggesting that the TASK positivity is a general feature of the astrocytes, and not a specific feature of the cerebellar astrocytes only (for the cochlear nucleus see the insets of fig. 2A–C, for hippocampus see fig. 3).

The expression of TASK-1, -2 and -3 in cerebellar astrocyte cultures was also confirmed by RT-PCR and Western blotting. As seen in figure 4, all channels investigated were expressed both at the mRNA (fig. 4A) and at the protein (fig. 4B) levels.

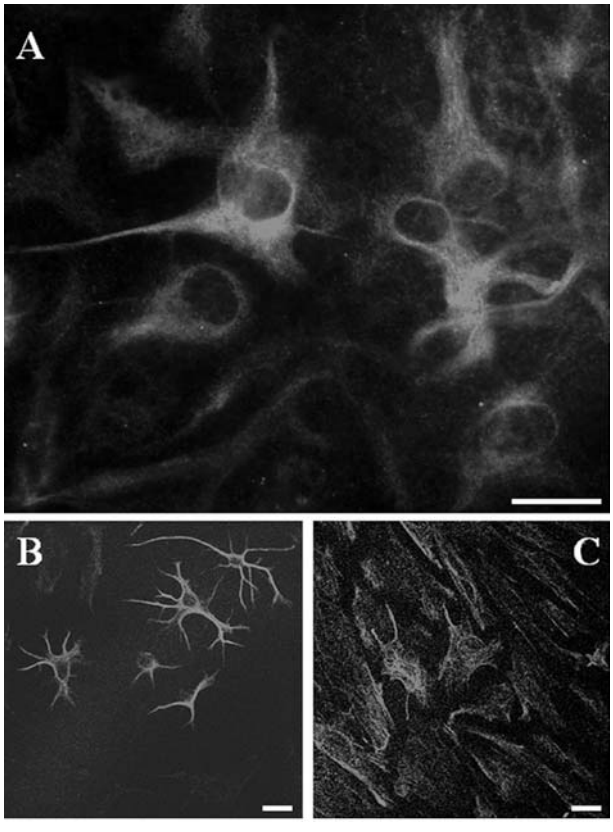


Figure 3. TASK immunolabelling of cultured hippocampal astrocytes of the rat. High-magnification image acquired with an immunofluorescent microscope, where the fine structure of the intracellular TASK-3-specific labelling is clearly visible (*A*). Confocal microscope images for TASK-1 (*B*) and TASK-2 (*C*). Both were taken in a plane which ran at about half the total height of the cells. Scale bars; 20 µm.

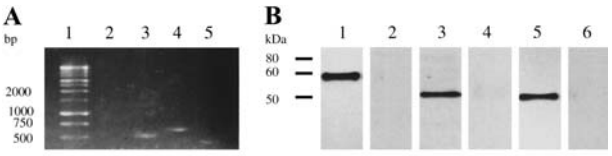


Figure 4. Expressions of TASK-1, -2 and -3 in cultured cerebellar astrocytes. (*A*) RT-PCR analysis of TASK-1, -2 and -3 mRNA expression in cultured cerebellar astrocytes. Lane 1, nucleotide standard (base pair, bp); lane 2, non-template control; lane 3, TASK-1; lane 4, TASK-2; lane 5, TASK-3. (*B*) Western blot analysis of TASK-1, -2 and -3 protein expression in cultured cerebellar astrocytes. Cells were harvested, similar amounts of protein were subjected to SDS-PAGE, and Western immunoblotting was then performed using goat antibodies as described in Materials and methods. Lanes 1, 3 and 5, TASK-1, TASK-2 and TASK-3, respectively; lanes 2, 4 and 6; same primary antibodies but in the presence of TASK-1, -2 and -3-specific blocking peptides, respectively. The blocking peptide concentrations were 7 µg/ml for TASK-1 and TASK-2, 20 µg/ml for TASK-3. The expected molecular size is approximately 60 kDa for TASK-1 and approximately 50 kDa for TASK-2 and TASK-3. Two additional sets of experiments gave in similar results.

**TASK-channels are most likely expressed in the ER of astrocytes**

Figure 3 demonstrates a very intriguing feature of the TASK expression of the astrocytes (this time yielded from the hippocampus). Figure 3A shows a high-magnification image produced by an immunfluorescence microscope, where a very fine, filament-like distribution of the TASK-3 immunopositivity is clearly visible, which apparently spares the nucleus of the cell. This pattern raised the possibility that besides the surface membrane of the astrocytes, all three investigated types of TASK channel may be present intracellularly, perhaps linked to the ER. Two techniques were utilised to confirm this possibility. Figure 3B, C demonstrate two confocal microscope images, taken in a horizontal plane which runs at about the middle of the total depth of the cells (4 µm from the bottom of the astrocyte), where anti-TASK-1 (fig. 3B) or anti-TASK-2 (fig. 3C) antibodies were used. As can be seen, the immunopositivity was not confined to the surface of the cells, but was also present intracellularly.

In the next step, a more direct approach was utilised to confirm the intracellular presence of the TASK channels. In these experiments, the cultured astrocytes (obtained from the hippocampus) were transfected with the pDsRed2-ER plasmid, whose protein product is localised in the ER of the transfected cells, and whose presence can be demonstrated by showing its red fluorescence 24 h after the transfection (fig. $5A_1$). As figure $5A_4$ shows, not all cells expressed the protein, while figure $5A_2$ demonstrates the results of the control experiment, where the cells were treated with the

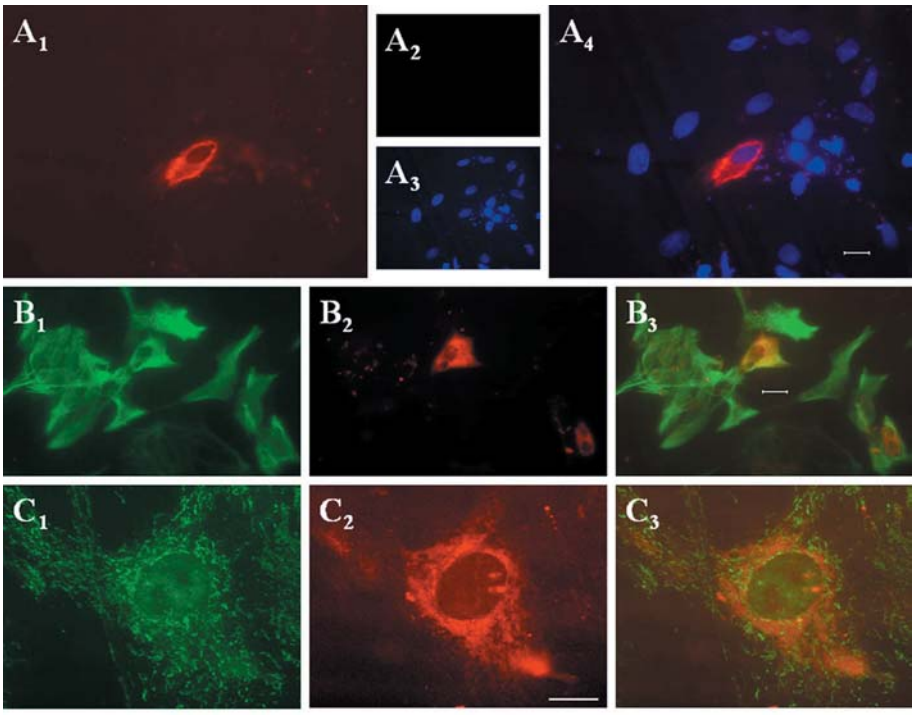


Figure 5. Colocalisation of the TASK channels and the protein product of the pDsRed2-ER plasmid in cultured hippocampal astrocytes. (*A1*) Image of a cultured astrocyte where transfection with the ER-specific vector was successful, as indicated by the red fluorescence. (*A4*) Same field of view, where the DAPI labelling of the nuclei (blue) is also visible. Note the other cells where the transfection was not successful. (*A2*) An image acquired from a cover-slip, where only the solvent of the plasmid was employed. (*A3*) The same field of view with DAPI labelling visible. (*B1*) TASK-1-specific immunoreaction on cultured hippocampal astrocytes. (*B2*) Same field of view but the product of the pDsRed2-ER plasmid is visible. (*B3*) Co-localisation image. (*C*) As for *B* but with TASK-2 specific labelling and higher magnification. Scale bars, 20 µm.

solvent of the plasmid only. Figure 5$A_3$ demonstrates the cell nuclei (DAPI) found in the same region. Twenty-four hours after the transfection, TASK-specific immunoreactions were performed, and the results of the TASK-1- (fig. 5$B_1$) and TASK-2- (fig. 5$C_1$) specific reactions are shown. Figure 5$B_2$, 5$C_2$ present the red immunofluorescence of the same regions, while figure 5$B_3$, $C_3$ are the co-localisation images. The orange colour observed here indicates co-localisation, suggesting that the TASK channels of the astrocytes are not only expressed on the surface membrane, but are also present in the ER. Similar results were obtained when TASK-3 expression was investigated in the same way (data not shown). To quantify the co-localisation, a pixel analysis was performed, where the percentage of pixels showing both green (TASK isoform) and red (DsRed2-ER) positivity was determined, relative to the number of all green pixels. The results showed that in the case of TASK-1, 48 ± 12% of the green (TASK-labelled) pixels were red too. For TASK-2, 25 ± 7% of the green pixels were red as well; while after the TASK-3 reaction, 23 ± 11% of the green pixels showed red fluorescence (n = 5 in each case; mean ± SE; the cells were selected from different staining runs).

**TASK-specific immunopositivity in the human cerebellum**

After checking for the distribution of the TASK-1, -2 and -3 immunoreactivities in the rat cerebellum, a similar study was conducted in the human cerebellum (fig. 6). In the case of the TASK-1 immunoreaction (fig. 6A), the distribution pattern was similar to that observed in the rat; namely, the Purkinje cells and the pia mater showed strong positivity, and a somewhat weaker but nevertheless present immunoreaction could be found in the molecular and granule cell layers. As seen in figure 6C, the TASK-3 distribution was similar to that of TASK-1, but it appeared to be stronger in all regions. The TASK-3 positivity was particularly pronounced in the Purkinje cells and in the pia mater. Compared to the TASK-1 and TASK-3 immunoreactions, the TASK-2 immunopositivity of the human cerebellum was weak, and only the Purkinje and granule cells gave noticeable TASK-2 positivity.

The TASK channel expression of the human cerebellum was also tested using double immunolabelling, (fig. 7). As TASK-2 positivity was barely present, only the anti-TASK-1 and anti-TASK-3 antibodies were employed in these experiments, where the TASK-specific immunoreaction was combined with either NFP (fig. 7$A_1$, $B_1$) or GFAP (fig. 7$A_2$, $B_2$). In figure 7$A_1$, $B_1$ the strong anti-

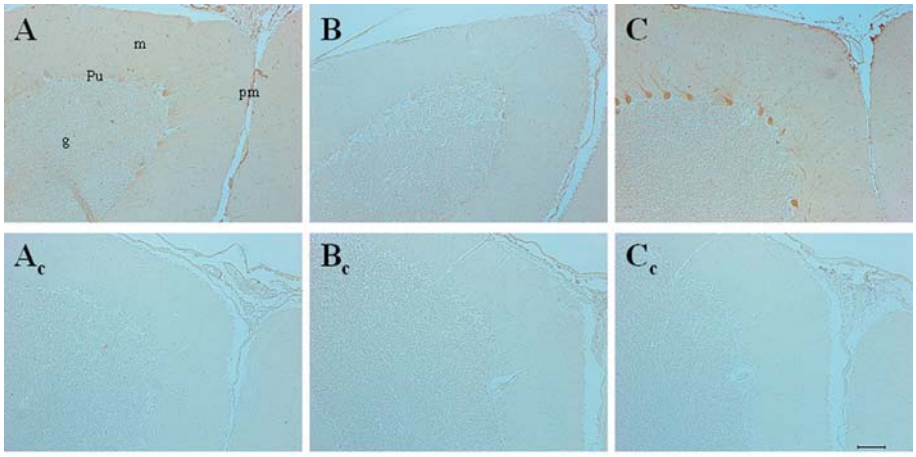


Figure 6. TASK-specific immunolabelling in the human cerebellum. Formalin-fixed, paraffin-embedded histological sections (4 µm) prepared from human cerebellum. TASK-1 (*A*), TASK-2 (*B*) and TASK-3 (*C*) immunolabelling. Immunoreaction when the TASK-1 ($A_C$), -2 ($B_C$) and -3 ($C_C$) specific primary antibodies were pre-incubated with their blocking peptides (blocking peptide concentration, 20 µg/ml). No counterstaining was employed. Scale bar, 100 µm. pm, pia mater; g, granule layer; m, molecular layer; Pu, Purkinje layer.

TASK-1 and anti-TASK-3 immunoreactions (brown) of the Purkinje cells are clearly visible, along with their positivity for NFP. The dendrites of the Purkinje cells were also TASK positive. Some smaller cells demonstrating strong NFP positivity were also visible in the molecular layer. These cells appeared to be TASK-1 positive, but they did not demonstrate a TASK-3 immunoreaction. Figure 7$A_2$, $B_2$ show the results when the TASK-1 and TASK-3 labelling were combined with a GFAP immunoreaction. The multi-processed, spider-like cells, with distinct positivity for GFAP also demonstrated TASK positivity. Worth noting is that the TASK-1 positivity of the astrocytes seemed to be stronger than their TASK-3 labelling, a finding in sharp contrast with the situation observed in the cases of the Purkinje cells.

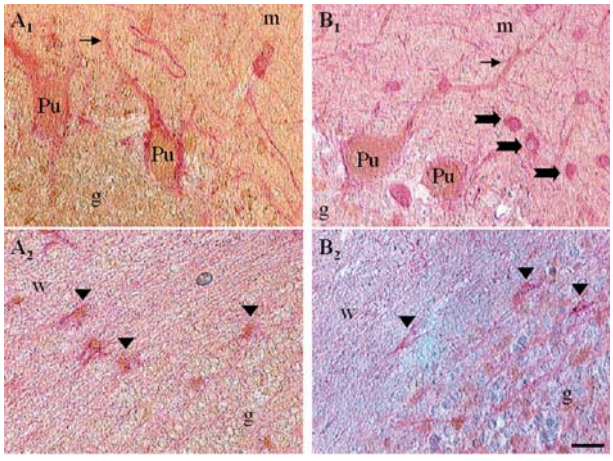


Figure 7. TASK-and-neurone as well as TASK-and-glia specific immunolabelling in the human cerebellum. Formalin-fixed histological sections (4 µm). TASK-1 specific immunoreaction ($A_1$, $A_2$) TASK-3-specific labelling ($B_1$, $B_2$) (brown). In all cases double-staining was performed. The TASK immunoreaction was combined with a neurone-specific labelling (anti-NFP reaction) ($A_1$, $B_1$), or with a glia-specific marker (anti-GFAP) ($A_2$, $B_2$). The neurone- and glia-specific reactions are purple. No counterstaining was applied in these cases. The pictures were taken using an oil-immersion objective with a magnification of × 60. Scale bar, 20 µm. g, granule layer; m, molecular layer; w, white matter; Pu, Purkinje cell. Thin arrows in $A_1$ and $B_1$ demonstrate the clearly visible processes of Purkinje cells. The thick arrows in $B_1$ show NFP-positive cells in the molecular layer, which do not demonstrate TASK immunopositivity. The arrowheads in $A_2$ and $B_2$ demonstrate GFAP-positive astrocytes showing simultaneous TASK positivity.

## Discussion

This study investigated the distribution of the TASK-specific immunoreaction, primarily in the rat and human cerebellum. Our results with the TASK-1 immunoreactivity were effectively the same as those reported in an earlier study [30], validating the experimental methods we employed. The distribution of the TASK-2 immunoreactivity found in our study was also very similar to that reported earlier [31]. However, in contrast to this earlier report, we demonstrated a weak but nevertheless present TASK-2 positivity of the astrocytes. However, to the best of our knowledge, this is the first study to report on the distribution of TASK-3 immunopositivity in the rat cerebellum, and we are the first to present data concerning the TASK-1, -2 and -3 patterns of the human cerebellum. Our work shows that the astrocytes not only express TASK channels in situ, but they maintain their ability to do so in tissue culture as well. The presence of TASK channels on the astrocytes further emphasises their functions in the $K^+$ handling of the central nervous system. Some of our results also raise the possibility that a significant number of TASK channels are present in the ER. Further studies are required, however, to determine whether these channels

are only produced here or whether they are expressed in the ER and trafficked between the ER and the surface membrane as suggested in the cases of TASK-1-transfected COS cells [39].

Similar to a study published earlier [30], strong TASK-1 positivity was noticed in the rat Purkinje cells, while a somewhat milder but definite immunoreaction was seen in the molecular and granular layers of the cerebellar hemispheres. The pia mater also proved to be strongly TASK-1 positive. Strong TASK-1 positivity of the glial cells of the cerebellum was reported in both studies. Moreover, similar to the findings of Millar et al. [25] who demonstrated the presence of TASK-1 immunoreactivity on cultured granule cells and astrocytes isolated from the cerebellum of the rat, we could also demonstrate that the astrocytes of the rat cerebellum, hippocampus and cochlear nucleus showed TASK-1 positivity. TASK-1 channel expression has previously been suggested in the cochlear nucleus [40], but no information about the expression pattern at the cellular level has been provided, and whether the glial cells of the cochlear nucleus also express TASK-1 channels has also not yet been demonstrated. Our results also showed that both the GluR and GluT types of astrocytes [38] expressed TASK-1 channels.

The results regarding the distribution of the TASK-2 channels in the rat cerebellum are also very similar to those reported earlier [31]. More specifically, Purkinje cells showed the strongest positivity for TASK-2, while the immunoreaction was somewhat lower in the granular and molecular layers. However, the immunopositivity of the Purkinje cells was less intense in the present work. The reason for this discrepancy is not clear, although we cannot exclude the possibility that the counterstaining applied in our case reduced the intensity of the immunolabelling. In the absence of counterstaining (see fig. $1B_2$), the TASK-2-specific immunoreaction observed in the rat cerebellum appeared to be stronger. Moreover, in contrast to the results published before, we found TASK-2 positivity in astrocytes, although it was much less pronounced than their TASK-1 immunoreactivity. As this result was definitely different from those published previously, particular emphasis was laid upon the confirmation of our findings, and several lines of evidence indicate that the immunoreaction we found was real and not an artifact:

1) The FITC- and DAB-conjugated immunoreactions gave identical results. Moreover, when the primary antibody was omitted, no immunoreaction could be observed, indicating that the immunostaining reported here was not the result of aspecific binding of the secondary antibodies.
2) Two different anti-TASK-2 primary antibodies, obtained from different companies, were employed, and both gave positive and specific immunoreactions.
3) When the primary antibody obtained from either company was pre-incubated with its blocking peptide, the intensity of the immunoreaction was markedly reduced.
4) The regional differences observed in the intensity of the immunoreaction also suggested a specific rather than aspecific immunostaining.
5) The other techniques employed (Western blot, RT-PCR) confirmed the immunochemical results.

What, therefore, might be the possible reason for the discrepancy between our findings and those published earlier? Although the expression of TASK-1 channels shows some correlation with the development of the tissue [41], this is not likely to be the reason of the difference, because we investigated both adult and young animals, with identical results (unpublished observations). Although we cannot exclude that the different strain of rats used by the two laboratories (Sprague-Dawley vs Wistar) might explain the different results, it seems unlikely. There is one very important issue, however, which should be taken into consideration and may well explain the discrepancy. When the TASK-specific immunoreactions were investigated, several AR techniques were tried out in our study, to achieve the best result [as suggested in ref. 42]. These trials clearly showed that it was essential to use some sort of AR method was essential in the cases of paraformaldehyde-fixed tissue slices to obtain good and convincing immunolabelling. When the immunreaction was tried on tissue samples which were not exposed to AR, it gave a significantly weaker reaction. We cannot exclude the possibility, therefore, that the difference noticed in the TASK-2 positivity of the astrocytes was the result of the different AR methods applied by the two laboratories.

In their comprehensive and indeed very thorough study, Karschin et al. [40] did not report on the TASK-1- and TASK-3-specific in situ hybridisation reaction in either the Purkinje cells or the molecular layer of the cerebellum, despite the fact that strong TASK-1 immunopositivity was found for both structures when the immunoreaction against the protein product was investigated in both a paper by Kindler et al. [30] and in our work. The explanation of this discrepancy remains unclear.

As for the human expression of TASK channels in the cerebellum, our results are in very good agreement with the observations of Medhurst et al. [27]. They found that the TASK-3-specific mRNA has the most significant expression in the human cerebellum, the quantity of the TASK-1-specific mRNA is somewhat lower, although still significant, while TASK-2-specific mRNA had the lowest level. Despite the fact that the quantity of the mRNA may not necessarily be the same as the amount of the protein product, the correlation between our immunohistochemistry results and the previously reported RT-PCR data is noteworthy.

A particularly noteworthy observation in our study is that the distribution of the TASK-1, -2 and -3 channels is not necessarily identical, either within the cerebellum, or between human and rat. Although such a discrepancy between the TASK-1/3 and TASK-2 immunoreactivity is not very surprising, since TASK-2 is remotely related to the TASK-1 and TASK-3 channels (which, on the other hand, are close relatives with 59.2% homology [15, 16, 43, 44]), the difference observed between the TASK-1 and TASK-3 distribution seems to be more exciting. For example, in rats, the pia mater showed strong TASK-1 positivity along with the lack of a TASK-3 immunoreaction. Further studies are required, however, to determine the functional significance of the differential distribution of TASK-1 and TASK-3 channels.

Moreover, when the distribution patterns of the TASK channels in the rat and human cerebellum were compared, some interesting interspecies differences seemed to emerge. While in the rat cerebellum, the TASK-1 positivity was the strongest, in humans, TASK-3 seemed to be more significantly expressed. We also noted that the Purkinje cells of the rat were strongly positive for TASK-2, while the human Purkinje cells did not show particularly prominent TASK-2 positivity, although it was definitely present. Moreover, unlike the rat pia mater which showed strong TASK-1 immunopositivity, and no TASK-3 immunoreactivity at all, in the human brain, the TASK-3 channels seemed to dominate, while the significance of the TASK-1 channels appeared to be less pronounced. In the light of a recent paper [45], the strong TASK-1 and TASK-3 positivity of the human cerebellum (particularly at the level of the Purkinje cells) might suggest that in addition to the homomeric channel formation, TASK-1/TASK-3 heteromers are formed in the human central nervous system.

*Acknowledgements.* This work was supported by grants from the Hungarian Science Foundation (13B0-0/19/TS01, F035036, TS040773 and T046067) and OMFB (00200/2002). The authors are grateful to Mrs. T. Kálmánczy and Mrs. E. Károlyi for their excellent and truly professional work on the tissue sections, and to Mrs. I. Varga for her general technical assistance. We also wish to thank the generous help of Ms. E. Bodó, Dr. J. Lázár and Dr. Z. Griger in the Western blotting and RT-PCR.

1 Rudy B. (1988) Diversity and ubiquity of K channels. Neuroscience **25:** 729–749
2 Coetzee W. A., Amarillo Y., Chiu J., Chow A., Lau D., McCormack T. et al. (1999) Molecular diversity of $K^+$ channels. Ann. N. Y. Acad. Sci. **868:** 233–285
3 Ketchum K. A., Joiner W. J., Sellers A. J., Kaczmarek L. K. and Goldstein S. A. (1995) A new family of outwardly rectifying potassium channel proteins with two pore domains in tandem. Nature **376:** 690–695
4 Lesage F., Guillemare E., Fink M., Duprat F., Lazdunski M., Romey G. et al. (1996) TWIK-1, a ubiquitous human weakly inward rectifying $K^+$ channel with a novel structure. EMBO J. **15:** 1004–1011
5 Chavez R. A., Gray A. T., Zhao B. B., Kindler C. H., Mazurek M. J., Mehta Y. et al. (1999) TWIK-2, a new weak inward rectifying member of the tandem pore domain potassium channel family. J. Biol. Chem. **274:** 7887–7892
6 Patel A. J., Maingret F., Magnone V., Fosset M., Lazdunski M. and Honore E. (2000) TWIK-2, an inactivating 2P domain $K^+$ channel. J. Biol. Chem. **275:** 28722–28730
7 Fink M., Duprat F., Lesage F., Reyes R., Romey G., Heurteaux C. et al. (1996) Cloning, functional expression and brain localization of a novel unconventional outward rectifier $K^+$ channel. EMBO J. **15:** 6854–6862
8 Patel A. J., Honore E., Maingret F., Lesage F., Fink M., Duprat F. et al. (1998) A mammalian two pore domain mechano-gated S-like $K^+$ channel. EMBO J. **17:** 4283–4290
9 Bang H., Kim Y. and Kim D. (2000) TREK-2, a new member of the mechanosensitive tandem-pore $K^+$ channel family. J. Biol. Chem. **275:** 17412–17419
10 Lesage F., Terrenoire C., Romey G. and Lazdunski M. (2000) Human TREK2, a 2P domain mechano-sensitive $K^+$ channel with multiple regulations by polyunsaturated fatty acids, lysophospholipids, and Gs, Gi, and Gq protein-coupled receptors. J. Biol. Chem. **275:** 28398–23405
11 Fink M., Lesage F., Duprat F., Heurteaux C., Reyes R., Fosset M. et al. (1998) A neuronal two P domain $K^+$ channel stimulated by arachidonic acid and polyunsaturated fatty acids. EMBO J. **17:** 3297–3308
12 Duprat F., Lesage F., Fink M., Reyes R., Heurteaux C. and Lazdunski M. (1997) TASK, a human background $K^+$ channel to sense external pH variations near physiological pH. EMBO J. **16:** 5464–5471
13 Leonoudakis D., Gray A. T., Winegar B. D., Kindler C. H., Harada M., Taylor D. M. et al. (1998) An open rectifier potassium channel with two pore domains in tandem cloned from rat cerebellum. J. Neurosci. **18:** 868–877
14 Kim Y., Bang H. and Kim D. (1999) TBAK-1 and TASK-1, two-pore $K^+$ channel subunits: kinetic properties and expression in rat heart. Am. J. Physiol. **277:** H1669–H1678
15 Kim Y., Bang H. and Kim D. (2000) TASK-3, a new member of the tandem pore $K^+$ channel family. J. Biol. Chem. **275:** 9340–9347
16 Rajan S., Wischmeyer E., Xin Liu G., Preisig-Muller R., Daut J., Karschin A. et al. (2000) TASK-3, a novel tandem pore domain acid-sensitive $K^+$ channel. An extracellular histidin as pH sensor. J. Biol. Chem. **275:** 16650–16657
17 Kim D. and Gnatenco C. (2001) TASK-5, a new member of the tandem-pore $K^+$ channel family. Biochem. Biophys. Res. Commun. **284:** 923–930
18 Ashmole I., Goodwin P. A. and Stanfield P. R. (2001) TASK-5, a novel member of the tandem pore K+ channel family. Pflügers Arch. **442:** 828–833
19 Reyes R., Duprat F., Lesage F., Fink M., Salinas M., Farman N. et al. (1998) Cloning and expression of a novel pH-sensitive two pore domain $K^+$ channel from human kidney. J. Biol. Chem. **273:** 30863–30869
20 Girard C., Duprat F., Terrenoire C., Tinel N., Fosset M., Romey G. et al. (2001) Genomic and functional characteristics of novel human pancreatic 2P domain $K^+$ channels. Biochem. Biophys. Res. Commun. **282:** 249–256
21 Decher N., Maier M., Dittrich W., Gassenhuber J., Bruggemann A., Busch A. E. et al. (2001) Characterization of TASK-4, a novel member of the pH-sensitive, two-pore domain potassium channel family. FEBS Lett. **492:** 84–89
22 Rajan S., Wischmeyer E., Karschin C., Preisig-Muller R., Grzeschik K. H., Daut J. et al. (2001) THIK-1 and THIK-2, a novel subfamily of tandem pore domain $K^+$ channels. J. Biol. Chem. **276:** 7302–7311
23 Sano Y., Inamura K., Miyake A., Mochizuki S., Kitada C., Yokoi H. et al. (2003) A novel two-pore domain $K^+$ channel, TRESK, is localized in the spinal cord. J. Biol. Chem. **278:** 27406–27412

24 Watkins C. S. and Mathie A. (1996) A non-inactivating $K^+$ current sensitive to muscarinic receptor activation in rat cultured cerebellar granule neurons. J. Physiol. **491:** 401–412
25 Millar J. A., Barratt L., Southan A. P., Page K. M., Fyffe R. E., Robertson B. et al. (2000) A functional role for the two-pore domain potassium channel TASK-1 in cerebellar granule neurons. Proc. Natl. Acad. Sci. USA 97: 3614–3618
26 Lauritzen I., Zanzouri M., Honoré E., Duprat F., Ehrengruber M. U., Lazdunski M. et al. (2003) $K^+$-dependent cerebellar granule neuron apoptosis. J. Biol. Chem. **278:** 32068–32076
27 Medhurst A. D., Rennie G., Chapman C. G., Meadows H., Duckworth M. D., Kelsell R. E. et al. (2001) Distribution analysis of human two pore domain potassium channels in tissues of the central nervous system and periphery. Brain Res. Mol. Brain. Res. **86:** 101–114
28 Pei L., Wiser O., Slavin A., Mu D., Powers S., Jan L. Y. et al. (2003) Oncogenic potential of TASK3 (Kcnk9) depends on $K^+$ channel function. Proc. Nat. Acad. Sci. USA. **100:** 7803–7807
29 Mu D., Chen L., Zhang X., See L-H., Koch C. M., Yen C. et al. (2003) Genomic amplification and oncogenic properties of the KCNK9 potassium channel gene. Cancer Cell. **3:** 297–302
30 Kindler C. H., Pietruck C., Yost C. S., Sampson E. R. and Gray A. T. (2000) Localization of the tandem pore domain $K^+$ channel TASK-1 in the rat central nervous system. Brain Res. Mol. Brain. Res. **80:** 99–108
31 Gabriel A., Abdallah M., Yost C. S., Winegar B. D. and Kindler C. H. (2002) Localization of the tandem pore domain $K^+$ channel KCNK5 (TASK-2) in the rat central nervous system. Brain Res. Mol. Brain. Res. **98:** 153–163
32 Rusznák Z., Harasztosi C., Stanfield P. R. and Szücs G. (2001) An improved cell isolation technique for studying intracellular $Ca^{2+}$ homeostasis in neurones of the cochlear nucleus. Brain Res. Brain Res. Protoc. **7:** 68–75
33 Roderick H. L., Campbell A. K. and Llewellyn D. H. (1997) Nuclear localisation of calreticulin in vivo is enhanced by its interaction with glucocorticoid receptors. FEBS Lett. **405:** 181–185
34 Kendall J. M., Badminton M. N., Dormer R. L. and Campbell A. K. (1994) Changes in free calcium in the endoplasmic reticulum of living cells detected using targeted aequorin. Anal. Biochem. **221:** 173–181
35 Meuth S. G., Budde T., Kanyshkova T., Broicher T., Munsch T. and Pape H.-C. (2003) Contribution of TWIK-related acid-sensitive $K^+$ channel 1 (TASK1) and TASK3 channels to the control of activity modes in thalamocortical neurons. J. Neurosci. **23:** 6460–6469
36 Lázár J., Szabó T., Kovács L., Blumberg P. M. and Bíró T. (2003) Distinct features of recombinant vanilloid receptor-1 expressed in various expression systems. Cell. Mol. Life Sci. **60**: 2228– 2240
37 Laemmli U. K. (1970) Cleavage of structural proteins during the assembly of the head of bacteriophage T4. Nature **227:** 680–685
38 Matthias K., Kirchhoff F., Seifert G., Huttmann K., Matyash M., Kettenmann H. et al. (2003) Segregated expression of AMPA-type glutamate receptors and glutamate transporters defines distinct astrocyte populations in the mouse hippocampus. Neurosci. **23:** 1750–1758
39 Girard C., Tinel N., Terrenoire C., Romey G., Lazdunski M. and Borsotto M. (2002) p11, an annexin II subunit, an auxiliary protein associated with the background $K^+$ channel, TASK-1. EMBO J. **21:** 4439–4448
40 Karschin C., Wischmeyer E., Preisig-Muller R., Rajan S., Derst C., Grzeschik K. H. et al. (2001) Expression pattern in brain of TASK-1, TASK-3, and a tandem pore domain $K^+$ channel subunit, TASK-5, associated with the central auditory nervous system. Mol. Cell. Neurosci. **18:** 632–648
41 Brickley S. G., Revilla V., Cull-Candy S. G., Wisden W. and Farrant M. (2001) Adaptive regulation of neuronal excitability by a voltage-independent potassium conductance. Nature **409:** 88–92
42 Montero C. (2003) The antigen-antibody reaction in immunohistochemistry. J. Histochem. Cytochem. **51:** 1–4
43 Czirják G. and Enyedi P. (2002) Formation of functional heterodimers between the TASK-1 and TASK-3 two-pore domain potassium channel subunits. J. Biol. Chem. **277:** 5426–5432
44 Talley E. M. and Bayliss D. A. (2002) Modulation of TASK-1 (Kcnk3) and TASK-3 (Kcnk9) potassium channels: volatile anesthetics and neurotransmitters share a molecular site of action. J. Biol. Chem. **277:** 17733–17742
45 Kang D., Han J., Talley E. M., Bayliss D. A. and Kim D. (2004) Functional expression of TASK-1/TASK-3 heteromers in cerebellar granule cells. J. Physiol. **554:** 64–77